



# An in-depth understanding of complex karstic system evolutions of northwest Iran using stable isotopes ( $\delta^{18}\text{O}$ , $\delta^2\text{H}$ , and $\delta^{13}\text{C}$ ) and hydrochemical techniques

Hossein Mohammadzadeh<sup>1,2</sup> · Effat Eskandari<sup>2</sup>

Received: 20 November 2020 / Accepted: 2 September 2021

© The Author(s), under exclusive licence to Springer-Verlag GmbH Germany, part of Springer Nature 2021

## Abstract

In this study, main characteristics controlling the evolution of groundwater chemistry were assessed by employing hydrochemical methods along with environmental stable isotope ( $\delta^{18}\text{O}$ ,  $\delta^2\text{H}$ , and  $\delta^{13}\text{C}$ ) techniques in major and complex karstic resources in Paveh–Javanrud (PV–JR) area, northwest (NW) of Iran. Thirty-four water samples from caves, springs, and wells were collected during two seasons for major ions (cations and anions) as well as stable isotope investigations on December 2014 (wet season) and October 2015 (dry season). Additionally, nine samples were also acquired from monthly precipitation (January 2015 till November 2015) for isotopic analyses from PV climatology station. Determining meteoric water line of Paveh (PMWL,  $\delta^2\text{H} = 6.9 \delta^{18}\text{O} + 11.9$ ,  $R^2 = 0.97$ ) indicates that the origination of air masses of the region was found to be Mediterranean Sea. Hydrogeochemical investigations, on the other hand, indicated that three major formations including a pure limestone, Bistoun formation (JKb), and two limestones with some sort of impurities, i.e., Ilam–Sarvak (KII-KSv) and Goru (Gr.) affected the water resources of the region. Regarding  $\delta^{18}\text{O}$  and  $\delta^2\text{H}$  results, most of karstic resources are plotted near PMWL and represent depleted isotopic values due to recharging from high altitudes. Finally, carbon isotope investigation was also utilized to determine the main source of carbon which was found to be carbonate dissolution and C4 plants. Furthermore, the karst development type (less-, moderate-, and well-developed) of all formations were identified. Providing that isotopic findings are complementary to hydrochemical features, this study gives an in-depth understanding of vulnerable karstic terrains in NW Iran, which are highly important frameworks for effective water management.

**Keywords** Stable isotopes ( $\delta^2\text{H}$ ,  $\delta^{18}\text{O}$ , and  $\delta^{13}\text{C}$ -DIC) · Karst aquifer · Hydrochemistry · Local meteoric water line (LMWL) · Residence time of water

## Introduction

As the global groundwater extraction rate (about  $1500 \text{ km}^3$  per year) grows continuously (Döll et al. 2012) and is significantly higher than its natural recharging rate, the world may lose the most invaluable sources of accessible freshwater sooner than expected, which is less than 30% of the total freshwater in the globe (Gleick and Schneider 1996).

Knowing such critical facts as well as the ever-increasing water demand due to population growth and industrialization are enough for countries to efficiently preserve, monitor, and utilize the remained water reservoirs. Therefore, evaluating the main characteristics of the aquifers is indispensable and yet one of only scientific ways for better water management. Presently, more than ever, the risk of water depletion specially from karstic aquifers is stunningly high due to indulged exploitation of karstic groundwater as an easily accessible water resource for various usages in many regions (Jiang et al. 2018).

To evaluate the main processes in the water cycle and hydrogeological conditions (including age, origin, quality, residence time, and so forth), the use of hydrochemical methods and environmental stable isotopes (including  $\delta^{18}\text{O}$ ,  $\delta^2\text{H}$ , and  $\delta^{13}\text{C}$ -DIC) have been widely practiced in recent decades all over the world, exclusively in regions with

✉ Hossein Mohammadzadeh  
mohammadzadeh@um.ac.ir

<sup>1</sup> Groundwater and Geothermal Research Center (GRC), Water and Environment Research Institute, Ferdowsi University of Mashhad, Mashhad, Iran

<sup>2</sup> Department of Geology, Faculty of Science, Ferdowsi University of Mashhad, Mashhad, Iran

karstic resources (Mohammadzadeh and Heydarizad 2020; Ayadi et al. 2018; Han et al. 2010b, 2014; Mohammadzadeh and Aravena 2015; Sánchez et al. 2015). The evolution of water chemistry is mainly affected by natural processes such as water–rock interaction and water residence time (Appelo and Postma 2004), and as a result, hydrochemical studies can be utilized effectively to deliver highly accurate information about the recharging areas (Cane and Clark 1999; Mohammadzadeh and Eskandari 2018; Parisi et al. 2011a), type of flow path (Marques et al. 2010; Pavlovskiy and Selle 2015; Qin et al. 2017), evaluating mixing processes (Han et al. 2010a; Langmuir 1997), mean residence time assessment (Goldscheider and Drew 2014), water suitability, and detecting probable contaminations (Djabri et al. 2008; Kumar et al. 2014).

Naturally occurring environmental stable isotopes, particularly  $\delta^{18}\text{O}$  and  $\delta^2\text{H}$  known as “fingerprints” in the hydrological cycle (Clark 2015), are also usually exploited to obtain precious information such as recharging pattern (Sappa et al. 2018), the mean residence time of water (Mustafa et al. 2015), the recharging altitudes and seasons (Mohammadzadeh and Aravena 2015; O’driscoll et al. 2005), and the aquifer’s depth and flow type (Qin et al. 2017). Besides  $\delta^{18}\text{O}$  and  $\delta^2\text{H}$  isotopes,  $\delta^{13}\text{C}$ -DIC is another useful tracer that originates from organic material decomposition and/or carbonate mineral dissolution (Kanduč et al. 2012), which can be used for monitoring the carbon cycle in aquatic ecosystems (Xuan et al. 2020). Although anthropogenic activities could also affect the  $\delta^{13}\text{C}$ -DIC in urban areas (Barnes and Raymond 2009; Xuan et al. 2020), but in karstic lands,  $\delta^{13}\text{C}$ -DIC mainly emanates from carbonate minerals and bedrock weathering (Barešić and Harvatincić 2011; Florea 2010). In addition, the  $\delta^{13}\text{C}$ -DIC in spring’s water is mainly controlled by the geologic composition of the recharging area (Kanduč et al. 2012). In recent decades, carbon isotope investigations have also found a special place in water studies including karstic regions and for evaluating the main processes in the carbon cycle such as detecting recharging regions (Knierim et al. 2013), the exchange processes (Barth et al. 2003; Florea 2010; Grossman 1997; Jin et al. 2014), and calcite precipitation conditions (Barešić and Harvatincić 2011; Stumm et al. 1981).

Karstic terrains greatly contribute to the main source of water supply in many arid regions, which are required to be studied more precisely (Ozdemir and Nalbantcilar 2002). One of the most crucial issues in the arid and semi-arid areas, such as Iran, is water shortage due to population growth, industrialization, and decreasing precipitations; all of which have increased the groundwater depletion rate at an enormously growing pace. Generally, 11% of the geologic structure of Iran is covered by bicarbonate formations, in which 55.2% of such formations are located along the Zagros Mountain belt (ZMB) in northwest (NW) Iran.

Paveh (PV) and Javanrud (JR) regions are located next to ZMB in northwest–southeast (NW–SE) direction at the west of Kermanshah province. The activity of Zagros main fault and high precipitation amount has intensified karst developments in this region and created springs with high discharge rate [regarding Bil spring (Fig. S1a)] near to or more than  $4000 \text{ L s}^{-1}$ . Furthermore, the presence of several watery caves [including Quri Qale (Fig. S1g, h) and Kawat caves (Fig. S1e, f)] also proves the high rate of karst development. Groundwater resources in the PV–JR area represent the main water supply for various usages. Some of the main rivers in Iran and Iraq have been originated and passed through these areas (Osati et al. 2014). Despite having such an important role in the water supply of the region, only a few investigations on these resources were reported in the literature. For instance, the moisture source of precipitation of Kermanshah province was reported by the previous studies (Mohammadzadeh et al. 2020). Out of nearby places next to PV and JR, Hamamin and Ali developed the Sulaymaniyah meteoric water line (SMWL) in the Kurdistan region, Iraq (Hamamin and Ali 2013). In 2012, local meteoric water line (LMWL) of the Marivan area in North of the PV–JR was defined by Mohammadzadeh and Ebrahimpour (Mohammadzadeh and Ebrahimpour 2012). In 2005, the LMWL of the Alvand region, located in the southern direction of PV–JR, had been developed by Karimi et al. (Karimi et al. 2005).

Bearing in mind that comprehensive investigations and use of multiple tracers and methods are pivotal for karstic terrains in arid and semi-arid regions, the water resources in the PV–JR area have not been studied systematically so far by isotopic and hydrochemical techniques. Therefore, the main aim of this study is to unravel the main features of the PV–JR complex karstic region through identifying the origin of water, evaluating the main factors affecting groundwater hydrochemistry, and monitoring stable isotopes of  $\delta^{18}\text{O}$ ,  $\delta^2\text{H}$ , and  $\delta^{13}\text{C}$ . The results of the study will enhance the understanding of the complex karstic system which would potentially lead to efficient water preservation and management.

## Materials and methods

### Study area

As shown in Fig. 1a,b, the region under study consists of Paveh (PV) and Javanrud (JR), which are located in the northeast (NE) of Kermanshah province near Iran and Iraq border, with geographical locations of  $46^{\circ}07'–46^{\circ}27' \text{N}$   $34^{\circ}75'–35^{\circ}18' \text{E}$  and  $45^{\circ}33'–55^{\circ}45' \text{N}$   $34^{\circ}51'–35^{\circ}04' \text{E}$ , respectively. PV–JR area comprises about  $1751 \text{ km}^2$  as a part of highly elevated and folded Zagros mountains

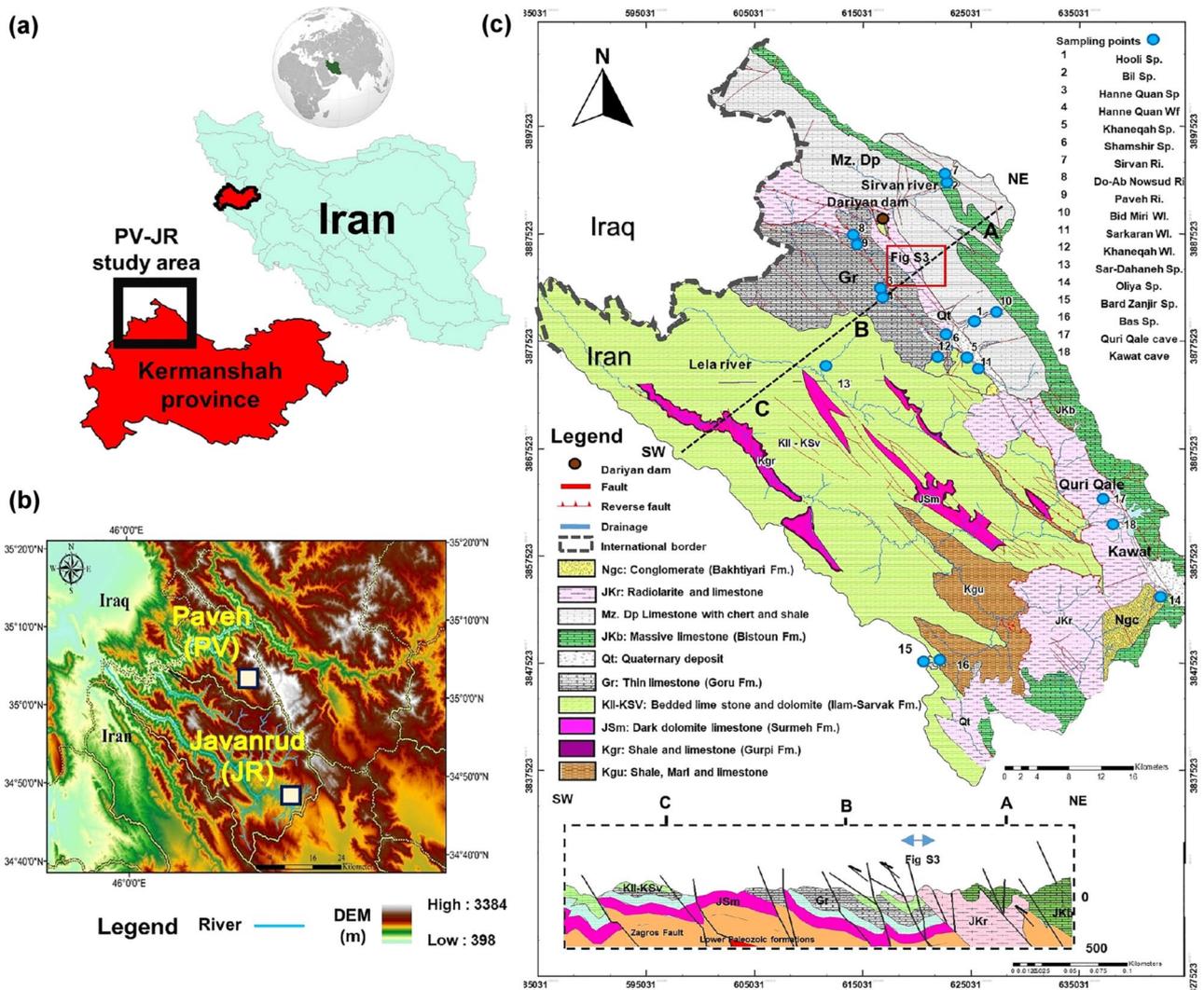


**Fig. 1** a The location of the study area, b digital elevation model (DEM), and c the geological map of PV–JR study areas. The geological cross-section is reproduced based on Sadeghi and Yassaghi (2016)

(Mohajjel and Fergusson 2014). The elevation ranges from 400 up to 3000 m.a.s.l (Fig. 1b). The mean annual precipitation of the area is about 653.7 mm and the average annual temperature is 14.8 °C. Calculated De Martonne aridity index of the area indicates that the region has a humid-moist and Mediterranean climate (Barati 2003). The rainfall season starts in winter, in which the most rainfalls occur in February, March, and April, while summer is the driest season of the region. The main moisture source of meteoric water originates from the Mediterranean and Black Seas in spring, whereas in other seasons, the Persian Gulf, the Red Sea, and the Arabian Sea air masses affect the climatic condition of the Kermanshah province (Mohammadzadeh et al. 2020). Since Zagros mountains receive up to 2000 mm of annual precipitation (Raziei et al. 2008), climatic conditions have also had an

important synergetic effect on the karst development in the region.

Large rivers in vicinity of Iran–Iraq border are mainly originated from the west of Iran (Raziei et al. 2008), such as the fifth largest one which is so-called the Sirvan river (Fig. S1b, c, d), moves across east to west of the region where finally enters into Iraq (Khazaei and Byzedi 2016). The land-use pattern of the area indicates that local forests cover most of the study area.

Major parts of the PV–JR region are covered by carbonate formations with noticeable tectonic activities and deformations due to Zagros main fault activities (Mohajjel and Fergusson 2014; Sadeghi and Yassaghi 2016). Radiolarite formation (JKr) (chert, shale, and impure limestone) from Jurassic-Cretaceous represent the oldest units in the northern part of the region, while Surmeh formation (JSm)

(limestone and dolomite) is the oldest unit and quaternary unconsolidated fan deposits are the youngest one (Fig. 1c). From the hydrogeological point of view, there are three important formations in the region. The Bistoun formation (JKb, pure limestone) is a karstic aquifer with a high rate of development in fractured zones and high discharge resources (i.e., Bil spring with  $4000 \text{ L s}^{-1}$ , and Bid Miri well with  $T = 772 \text{ m}^2 \text{ d}^{-1}$ ). Ilam-Sarvak formation (KII-KSv, limestone with gray marls and dolomite) and Goru formation (Gr, which is gray limestone and shale) are two other karstic aquifers, but due to having impurities, these formations have a lower discharge rate compared to Bistoun (JKb) water resources. The main direction of groundwater flow was found to be from east to west in PV area and from south-east to northwest in JR area which was determined based on some methods including the digital elevation model (DEM) of the study area and the direction of surface water in main rivers (Sirvan and Lela rivers) and groundwater discharge points (e.g., springs) (Fig. 1b, c), similar to a work reported by Morsali and Rezaei (Morsali and Rezaei 2017). So far, no comprehensive geological investigation has been carried out in the region and the only available information is a short report of geotechnical investigations in the northern part of the region, where the construction site of Dariyan dam (Fig. 1c) on the Sirvan River was ongoing at the time this study was undertaken.

## Sampling and analyses

Water resource samples for hydrochemistry and isotopic investigations were collected during two periods, December 2014 (wet season) and October 2015 (dry season). In this study, a total of 34 water samples were taken including ten karst springs, three wells, three rivers, and two watery caves (Fig. 1c). For the isotopic composition of precipitation, nine samples (seven rain and two snow samples) were collected from January 2015 till November 2015 at the PV city climatology station. Precipitation samples were collected after each precipitation event and samples were immediately transferred into the monthly bottle. To be specific, samples were collected into one-liter high-density polyethylene bottles (Mohammadzadeh et al. 2020), and the air temperature was recorded simultaneously (see supplementary information, Table S4).

Physicochemical parameters including water temperature (T) and pH were recorded synchronously by a portable multi-parameter instrument (VWR SP90M5, Handel Multi-parameter) and TDS is the summation of cations and anions. Before carrying out on-site measurement, the multi-parameter was calibrated using standard solutions based on standard methods (Heald et al. 2007). The collected samples for hydrochemistry analyses and stable isotopes of  $\delta^{18}\text{O}$  and  $\delta^2\text{H}$  (both precipitation and water resource) were first filtered

by  $0.45 \mu\text{m}$  membrane filters and were kept in 25 mL polyethylene heavy dense bottles (noting that the container was rinsed with the filtered water of the sampling site). All the cationic samples were mixed with nitric acid to preserve the solution  $\text{pH} < 2$ . Finally, all samples were stored below  $4 \text{ }^\circ\text{C}$  and refrigerated until analyzed. Major cations ( $\text{Ca}^{2+}$ ,  $\text{Mg}^{2+}$ ,  $\text{Na}^+$ , and  $\text{K}^+$ ) were determined using inductively coupled plasma atomic emission spectroscopy (ICP-AES). Different anions including  $\text{F}^-$ ,  $\text{Cl}^-$ ,  $\text{SO}_4^{2-}$ , and  $\text{NO}_3^-$  were measured by the ion chromatography (IC) method. Bicarbonate concentration was calculated using the carbon isotope in relation to pH (Clark 2015). Hydrochemical analyses of the samples were done at the hydrogeochemistry laboratory at Ottawa University, Canada.

Stable isotope measurements of  $\delta^{18}\text{O}/\delta^2\text{H}$  were performed using a Los Gatos Research (LGR, USA) analyzer at the Environmental Isotope Laboratory of Waterloo University, Canada. Inorganic carbon concentration and carbon stable isotope samples were collected in 40 mL dark glass vials without any air space and sealed with capes. An analytical Total Carbon Analyser (TCA-Aurora Model 1030) was used to measure the carbon content of the samples, while the isotopic abundance of the carbon isotopes was revealed by Continues-Flow Isotope Ratio Mass Spectrometer (CF-IRMS, model delta plus XP Thermos Finnegan-Germany) at G.G. Hatch Stable Isotope Laboratory, University of Ottawa, Canada.  $\delta^{18}\text{O}$  and  $\delta^2\text{H}$  isotopic ratios are expressed as per mil (‰) unit of Vienna Standard Mean Ocean Water (VSMOW). Carbon isotopic ratio ( $\frac{^{13}\text{C}}{^{12}\text{C}}$ ) values are expressed using “ $\delta$ ” notation with respect to Vienna Pee Dee Belemnite (VPDB) in per mil (‰). The error band in the LGR analysis for stable isotopes was reported to be  $\pm 0.2$  and  $\pm 0.8$  ‰ for  $\delta^{18}\text{O}$  and  $\delta^2\text{H}$ , respectively. The analytical precision for carbon isotopes is  $\pm 0.2$  per mil, while for DIC concentration, it is 2%. The relative analytical error (E, %) of all the hydrochemical samples was within an acceptable range.

## Results and discussion

### Water chemistry

Physicochemical parameters and hydrochemistry data of water resources are tabulated in Tables S1 and S2 (see supplementary materials). The pH ranged between 7 and 8.2, which implies neutral-to-slightly alkaline water. Most of the samples showed pH increment during the dry season, except Hanne Quan waterfall and Khaneqah well. The pH variations could arise from changes in residence time, flow path, and the discharge of water (Parisi et al. 2011b). Field observations confirmed the disposal of unrefined urban wastewaters directly into Hanne Quan waterfall, which can potentially raise the pH values (to 8.2 or above) in

both periods. The concentrations of major ions were lower than the WHO permissible limit for drinking usage (WHO 1993). The  $\text{NO}_3^-$  concentration in all the samples except for the Sirvan river in the dry season; the  $\text{NO}_3^-$  concentration in all of the samples was lower than the WHO permissible limit for portable usages ( $50 \text{ mg L}^{-1}$ ). The reason for such a high nitrate concentration ( $101.4 \text{ mg L}^{-1}$ ) in Sirvan river is that the river was not recharged from Bill spring (with  $4000 \text{ L s}^{-1}$  discharge) during dry season. Besides, the existence of fish farming pools over the Sirvan River (Adeli 2013) could be another source of anthropogenic contamination, which caused a worsened water quality (Table S2). The lack of precipitation in the dry period can be enumerated as another major factor affecting the  $\text{NO}_3^-$  concentration.

Piper triangular diagram was used to identify the main hydrochemical type of water and the relationship between major ions for both wet and dry seasons (Fig. 2 a, b). As shown, all of the samples are placed in zone 1 due to the dominance of calcium type. Whereas, all of the anions are placed in zone 5, indicating that bicarbonate is the main anionic source. The central diamond plot suggests that all of the samples are gathered in one group which refers to origination from carbonate formations. Because of water–rock interactions through carbonate beds, the hydrochemical type of water is mainly  $\text{Ca}^{2+}$ -  $\text{HCO}_3^-$  and carbonate hardness exceeds 50%. Rivers are placed near the karstic resources in both periods, indicating that surface waters are recharged by groundwater.

Among the samples, Kawat cave represents an excessive  $\text{Mg}^{2+}$  concentration. The nearest geological cross-sections to Kawat cave location (Fig. 1c and Fig. S3a) indicate that Surmeh (JSm) strata (dolomite and limestone) are placed under Goru (Gr) formation, and thus, Surmeh dissolution could be the probable source of excessive  $\text{Mg}^{2+}$  in Kawat cave (Fig. S3c). There is no adjacent urban water pollution source (Farid and Baloch 2012), which could cause the excessive  $\text{Cl}^- + \text{SO}_4^{2-}$  concentration in Hanne Quan waterfall, and it refers to the rural disposal wastewater and sewage entering into this water resource (Fig. 2b).

According to TDS values for potable usages (Fig. 3), groundwater resources are categorized into two groups. The first group of samples (group 1) shows low TDS (less than  $300 \text{ mg L}^{-1}$ ), which could be the result of water passing through a well-developed karst system with short residence time. The second group of samples (group 2) represents higher TDS values ( $300\text{--}600 \text{ mg L}^{-1}$ ) and has a longer residence time in comparison to group 1. As mentioned by Freeze and Cherry, an increase in TDS refers to the longer residence time of water (Freeze and Cherry 1979). Therefore, TDS parameter was then utilized as a relative basis for comparing the water resources.

In the wet season, Khaneqah spring (Fig. 3 a, b and Fig. S2), which is a seasonal spring with low discharge, represents the highest TDS value ( $555.5 \text{ mg L}^{-1}$ ) and the longest residence time of water. This spring is located close to a local drainage named Shamshir River (Fig. S2) which is also affected by the surface water, leading to a high TDS value.

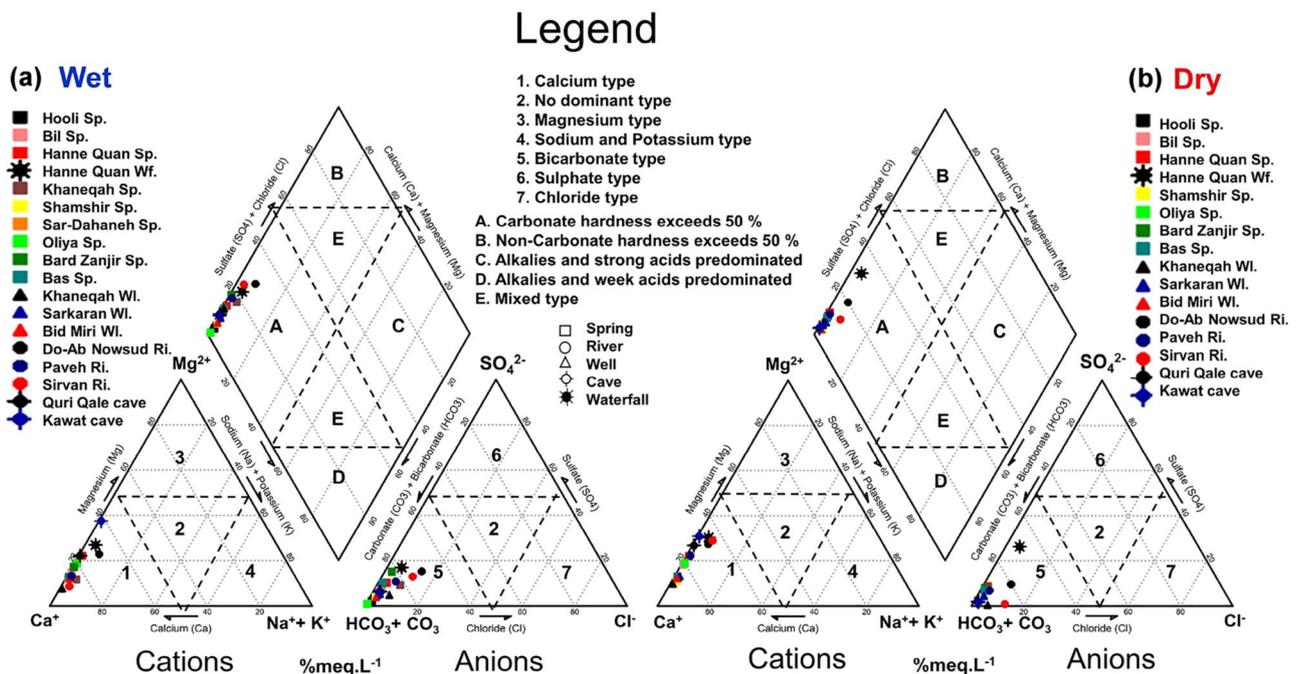
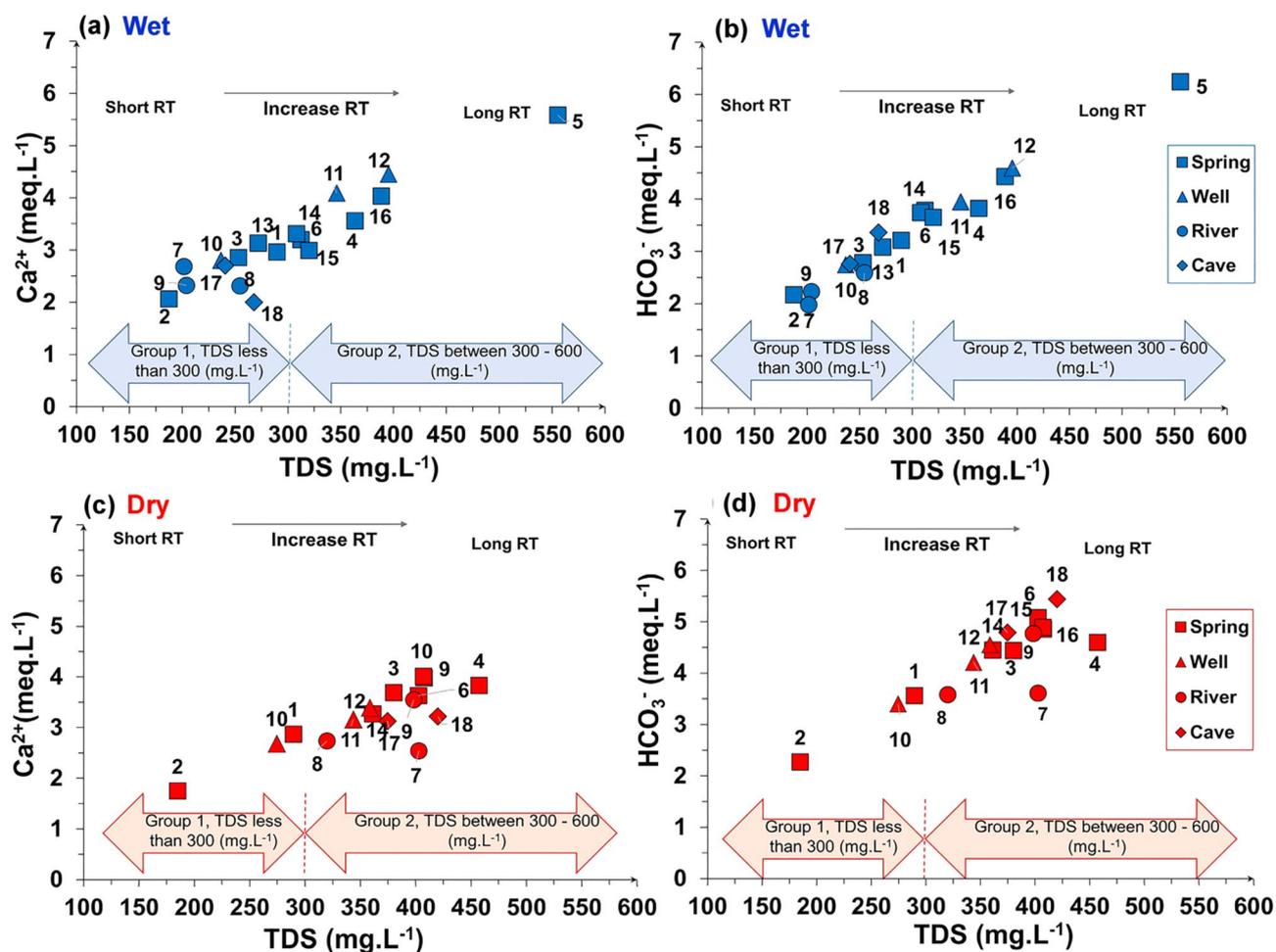


Fig. 2 Piper diagram of water reservoirs in (a) wet season and (b) dry season



**Fig. 3** The scatter plot of major ions ( $\text{Ca}^{2+}$  and  $\text{HCO}_3^-$ ) versus TDS in the (a and b) wet and (c and d) dry seasons. Note: site codes are presented in Table S1 and S2. RT Residence time. The reference for grouping is the Canadian Drinking Water Quality Guidelines (Toft

et al. 1987). Accordingly, the TDS is categorized as the flow for potable usages; excellent, less than  $300 \text{ mg L}^{-1}$  (group 1); good, between 300 and  $600 \text{ mg L}^{-1}$  (group 2)

Adversely, in both seasons, the Bil spring TDS value is low and the residence time of water is short (Fig. 3). The lack of precipitation in the dry season, though, has increased TDS in most resources (Fig. 3 c, d).

In general, three important formations affect the water quality of the area. First, Bistoun (JKb) formation samples represent the lowest average of TDS ( $297.0 \text{ mg L}^{-1}$ ), due to high karstic development [including Hooli (1), Bil (2), and Shamshir springs (6), Bid Miri (10), and Sarkaran well (11), Quri Qaleh (17), and Kawat cave (18)]. The Ilam–Sarvak formation is the second karstic aquifer which has moderate TDS ( $353 \text{ mg L}^{-1}$ ) [including Sar-Dahaneh (13), Oliya (14), Bas (15), and Bardzanjir springs (16)]. The Goru (Gr) formation with gray limes to black shales (Zarei et al. 2018) is the third karstic aquifer with the highest TDS average ( $368.0 \text{ mg L}^{-1}$ ) [including Hanne Quan spring (3), Hanne Quan waterfall (4), and Khaneqah well (5)], and a longer

residence time compared to JKb and KII-KSv aquifer (Table S1-S2 and Fig. 1c).

The correlation matrix of the physico-chemical parameter and major ions concentrations (Table 1) indicates that EC values have a proportional correlation with main ions in which dissolution of these ions increases the EC values. As carbonate formations dominate the region, the correlation between  $\text{Ca}^{2+}$  and  $\text{HCO}_3^-$  ( $r=0.81$ ) is significant. The  $\text{Mg}^{2+}$  correlation with  $\text{HCO}_3^-$  ( $r=0.38$ ) indicates that the dissolution of dolomite is less than that of calcite formations (Table 1).  $\text{Ca}^{2+}$  has a negative correlation with pH ( $r=-0.11$ ), since increasing the pH causes a decrease in the carbonate solubility in water.  $\text{Ca}^{2+}$  and  $\text{SO}_4^{2-}$  correlation ( $r=0.35$ ) may refer to gypsum or anhydrite dissolution.  $\text{Na}^+$  also shows an increasing ratio with  $\text{SO}_4^{2-}$  ( $r=0.57$ ), which could refer to the combined dissolution of halite and gypsum (Liu et al. 2019).

**Table 1** Correlation matrix of chemical parameters in the PV–JR study area

	T	pH	TDS	EC	K <sup>+</sup>	Na <sup>+</sup>	Mg <sup>2+</sup>	Ca <sup>2+</sup>	HCO <sub>3</sub> <sup>-</sup>	Cl <sup>-</sup>	NO <sub>3</sub> <sup>-</sup>	SO <sub>4</sub> <sup>2-</sup>
T	1.000											
pH	-0.481	1.000										
TDS	0.097	-0.022	1.000									
EC	0.310	-0.006	0.647	1.000								
K <sup>+</sup>	-0.364	0.182	-0.114	0.204	1.000							
Na <sup>+</sup>	-0.272	0.118	0.454	0.470	0.628	1.000						
Mg <sup>2+</sup>	-0.122	0.206	0.493	0.197	0.016	0.451	1.000					
Ca <sup>2+</sup>	0.261	-0.118	0.841	0.746	-0.156	0.255	0.182	1.000				
HCO <sub>3</sub> <sup>-</sup>	0.176	-0.103	0.948	0.525	-0.243	0.213	0.385	0.812	1.000			
Cl <sup>-</sup>	-0.383	0.152	0.403	0.578	0.630	0.852	0.232	0.297	0.189	1.000		
NO <sub>3</sub> <sup>-</sup>	-0.199	0.389	0.193	0.034	0.249	0.411	0.189	-0.128	0.011	0.350	1.000	
SO <sub>4</sub> <sup>2-</sup>	-0.113	0.185	0.382	0.445	0.475	0.571	0.544	0.357	0.199	0.422	-0.166	1.000

The Na<sup>+</sup>/Cl<sup>-</sup> ratio and Na<sup>+</sup>/Cl<sup>-</sup> 1:1 stoichiometry ratio line are depicted in Fig. 4a (wet season) and Fig. 4c (dry season). For Na<sup>+</sup>/Cl<sup>-</sup> ratio equals to one, halite (NaCl) dissolution is the major cause, while for the ratios higher than one, dissolution of Na-containing silicate material is the potential reason (Fisher and Mullican III 1997). Cl<sup>-</sup> could also emanate from evaporative minerals such as halite

and sylvite (KCl) (Freeze and Cherry 1979). According to Fig. 4a,c, most of the samples especially in the dry season plot over the 1:1 stoichiometric line and show an excessive Na<sup>+</sup>, which could be resulted from cation exchange processes in the aquifer and dissolution of Na-containing silicate minerals (e.g., Bakhtiyari conglomerate formation or Ngc seen from Fig. 1c). Whereas, in some samples, the

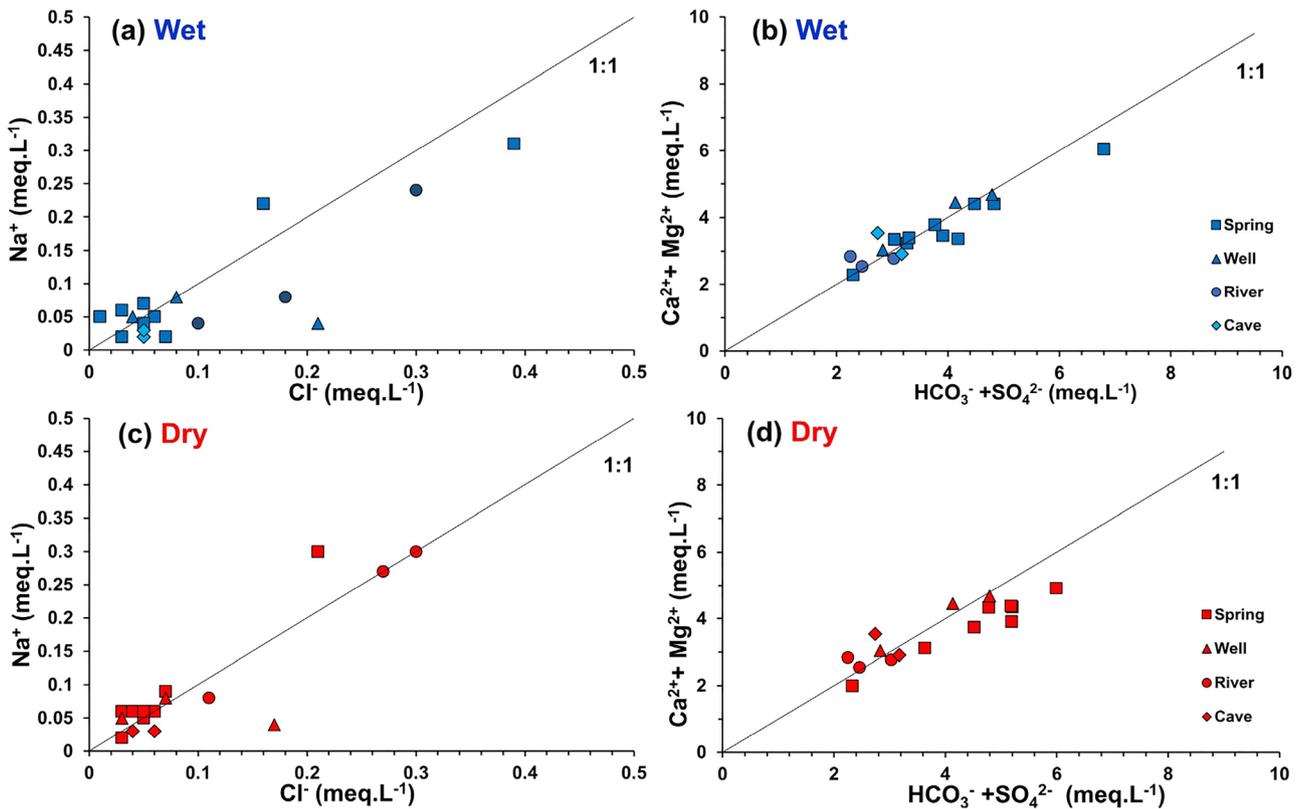


**Fig. 4** The scatter plot of Na<sup>+</sup> versus Cl<sup>-</sup> for (a) wet and (c) dry seasons, and scatter plot of Ca<sup>2+</sup> + Mg<sup>2+</sup> versus HCO<sub>3</sub><sup>-</sup> + SO<sub>4</sub><sup>2-</sup> for (b) wet and (d) dry seasons

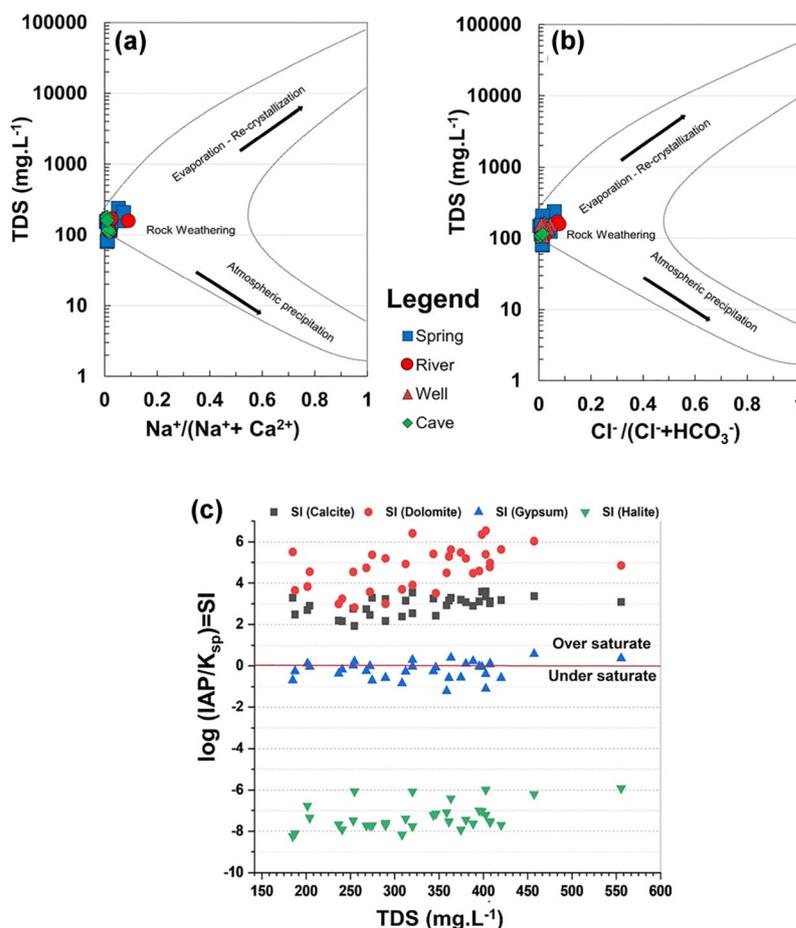
$\text{Na}^+/\text{Cl}^-$  ratio is less than one, which could refer to reverse ion exchange in the aquifer (Hounslow 2018).

The scatter plot of  $\text{Ca}^{2+} + \text{Mg}^{2+}$  against  $\text{HCO}_3^- + \text{SO}_4^{2-}$  for the wet and dry seasons (Fig. 4 b, d) was used to evaluate the carbonate and gypsum equilibrium. In water samples following the 1:1 line, carbonate and gypsum equilibrium mainly control these ions in the aquifer. Based on Belkhiri et al. (2011), the excess of  $\text{HCO}_3^- + \text{SO}_4^{2-}$  is a result of cation exchange and could shift the points to the right side. Reverse cation exchange, on the other hand, will increase the  $\text{Ca}^{2+} + \text{Mg}^{2+}$  and shift the samples to the left side (Belkhiri et al. 2011). As shown in Fig. 4 b, d, a few samples have excessive  $\text{Ca}^{2+}$  and  $\text{Mg}^{2+}$  and are plotted on the left side, while most of the samples are placed on the right side and represent an excess of  $(\text{HCO}_3^- + \text{SO}_4^{2-})$ , which is an indication of cation exchange (Belkhiri et al. 2011).

Gibbs diagram model (Gibbs 1970) exhibits that most of the samples are plotted in the rock weathering zone and the hydrochemistry of water is controlled by chemical weathering and mineral dissolution (Fig. 5 a, b).

The saturation indices (SI) with respect to calcite ( $\text{SI}_{\text{calcite}}$ ), dolomite ( $\text{SI}_{\text{dolomite}}$ ), gypsum ( $\text{SI}_{\text{gypsum}}$ ), and halite ( $\text{SI}_{\text{halite}}$ ) were calculated by PHREEQC computer code (Parkhurst 1995) (Fig. 5c and Table S3).  $\text{SI}_{\text{calcite}}$  values are ranged from 1.93 to 3.61, demonstrating that water resources are over-saturated due to carbonate minerals dominating the region.  $\text{SI}_{\text{dolomite}}$  ranges from 2.83 to 6.54. Even though the Mg concentration is low,  $\text{SI}_{\text{dolomite}}$  is supersaturated. The dissolution of dolomite from Quaternary sediments (Qt) and/or Bakhtiyari conglomerates (Ngc) increase the  $\text{Mg}^{2+}$  concentration in water. However, flowing of this water into limestone formations in turn increases  $\text{Ca}^{2+}$  and  $\text{CO}_3^{2-}$  concentrations in water through calcite dissolution and water will become supersaturated with respect to dolomite. Then, the subsequent slow dolomite precipitation reaction could be the possible mechanism for such a low Mg concentration in water samples (Fig. 5c) (Freeze and Cherry 1979). The SI values of gypsum and halite ranged between  $-1.21$  to  $0.58$  and  $-8.24$  to  $-5.95$ , respectively, indicating that the groundwater samples are under-saturated to slightly over-saturated with respect to gypsum, while all the samples are

**Fig. 5** Gibbs diagram: **a**  $\text{Na}^+(\text{Na}^+ + \text{Ca}^{2+})$  and **b**  $\text{Cl}^-(\text{Cl}^- + \text{HCO}_3^-)$  versus TDS. **c** Saturation indices of calcite, dolomite, gypsum, and halite versus TDS



under-saturated with respect to halite due to the dominance of carbonate formations.

Well-developed karstic resources of Bistoun formation (JKb) (eastern part of the area) represent low  $SI_{calcite}$  (average of 2.47). Whereas in the water samples of Ilam–Sarvak formation (KII-KSv),  $SI_{calcite}$  (average of 2.57) is slightly more than Bistoun formation (JKb). Goru formation (Gr) samples have higher  $SI_{calcite}$  (with an average of 3.06) than other formations. As water–rock interaction increment could increase the SI as well as TDS values, it can be concluded that water has a shorter mean residence time in Bistoun (JKb) resources due to lower water–rock interactions compared to Ilam–Sarvak (KII-KSv) and Goru formations (Gr) (Table S3).

### Local meteoric water lines (LMWLs) and the role of moisture sources on $\delta^{18}O$ and $\delta^2H$ compositions of precipitations

The average monthly precipitation in the PV climatology station is tabulated in Table S4. The mean values of  $\delta^{18}O$  and  $\delta^2H$  of meteoric water range from  $-7.2$  to  $-0.5\text{‰}$  and from  $-39.9$  to  $16.9\text{‰}$ , respectively. The Paveh meteoric water line (PMWL) is defined to be  $\delta^2H = 6.9 \delta^{18}O + 11.9$ ,  $R^2 = 0.97$  (Fig. 6). The slope of the PMWL is smaller than that of the global meteoric water line (GMWL), given by Craig (1961),  $\delta^2H = 8 \delta^{18}O + 10$ . (Craig 1961). Such a low value ( $< 8$ ) could be the result of low humidity (Gonfiantini et al. 1974), which causes an increase in evaporation (Clark 2015) and thus decreases the slope of PMWL to 6.9 (Fig. 6). The *d-excess* was used as an indicator to evaluate the origin of precipitation. Based on the results, the *d-excess* varies from 10.5 ‰ to 21.5 ‰ (Table S4), indicating that air masses have been derived from arid vapor sources (Florea and McGee 2010; Gat and Carmi 1987). As the eastern area of Mediterranean sea precipitations shows high values

of *d-excess* (Bershaw 2018), it can be inferred that prevailing air masses are mainly emanated from the vicinity of the Mediterranean Sea.

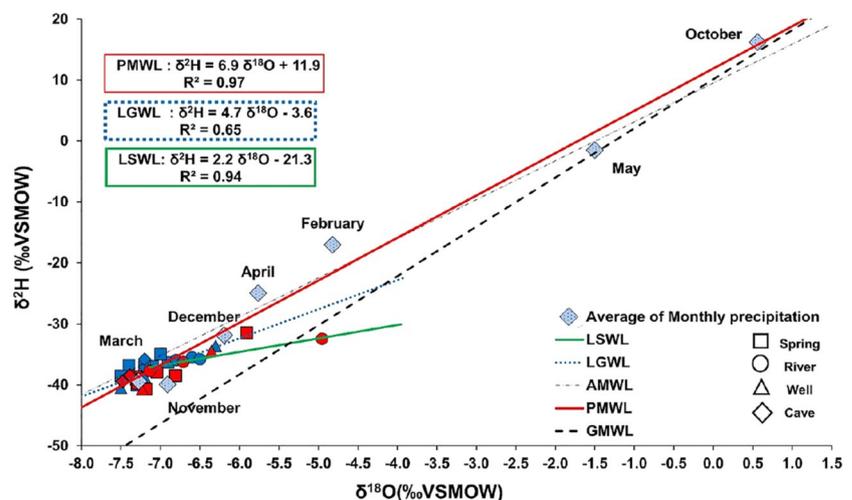
The relationship between  $\delta^{18}O$  isotope versus temperature and rain amount in the study area are given in Fig. S4a and S4b, respectively. As shown, the temperature has a much more significant effect on the isotopic fluctuation of oxygen according to its fitted regression line ( $R^2 = 0.65$ ).

### The composition of stable isotopes ( $\delta^2H$ and $\delta^{18}O$ ) in water resources

Based on the isotopic composition of water resources of PV–JR areas (Table S5), the majority of the samples are plotted close to the PMWL with some of them showing a degree of deviation from PMWL. This suggests that such water resources had mainly derived from meteoric precipitation, while they were affected by the evaporation effect. The local groundwater line (LGWL) was calculated as  $\delta^2H = 4.7 \delta^{18}O - 3.6$  ( $R^2 = 0.65$ ) and the surface local water line (LSWL) could be defined as  $\delta^2H = 2.2 \delta^{18}O - 21.3$  ( $R^2 = 0.94$ ). The LSWL follows a different trend due to a high degree of evaporation. Karstic resources represented a depleted isotopic content with high *d-excess* values. Among the water samples, rivers have enriched isotopic values due to evaporation, especially in the dry season (Fig. 7). Plotting  $\delta^{18}O$  and  $\delta^2H$  data simultaneously together with the PMWL and GMWL (Fig. 7 a, b) indicates that most of the samples are placed at the lower part of the PMWL. Most of the samples are placed near or on PMWL, indicating that recharged water was not affected by evaporation.

Water resources could be categorized into three groups based on the water origin. The first group of water resources recharges from Bistoun formation (JKb), with the average isotopic values of  $-7.3$  and  $-38.8 \text{‰}$  for  $\delta^{18}O$  and  $\delta^2H$ , respectively. High depletion isotope value proves that water

**Fig. 6** The relationship between  $\delta^{18}O$  and  $\delta^2H$  in precipitation, groundwater, and surface water. PMWL; GMWL (Craig 1961); AMWL (Karimi et al. 2005), LGWL, and LSWL



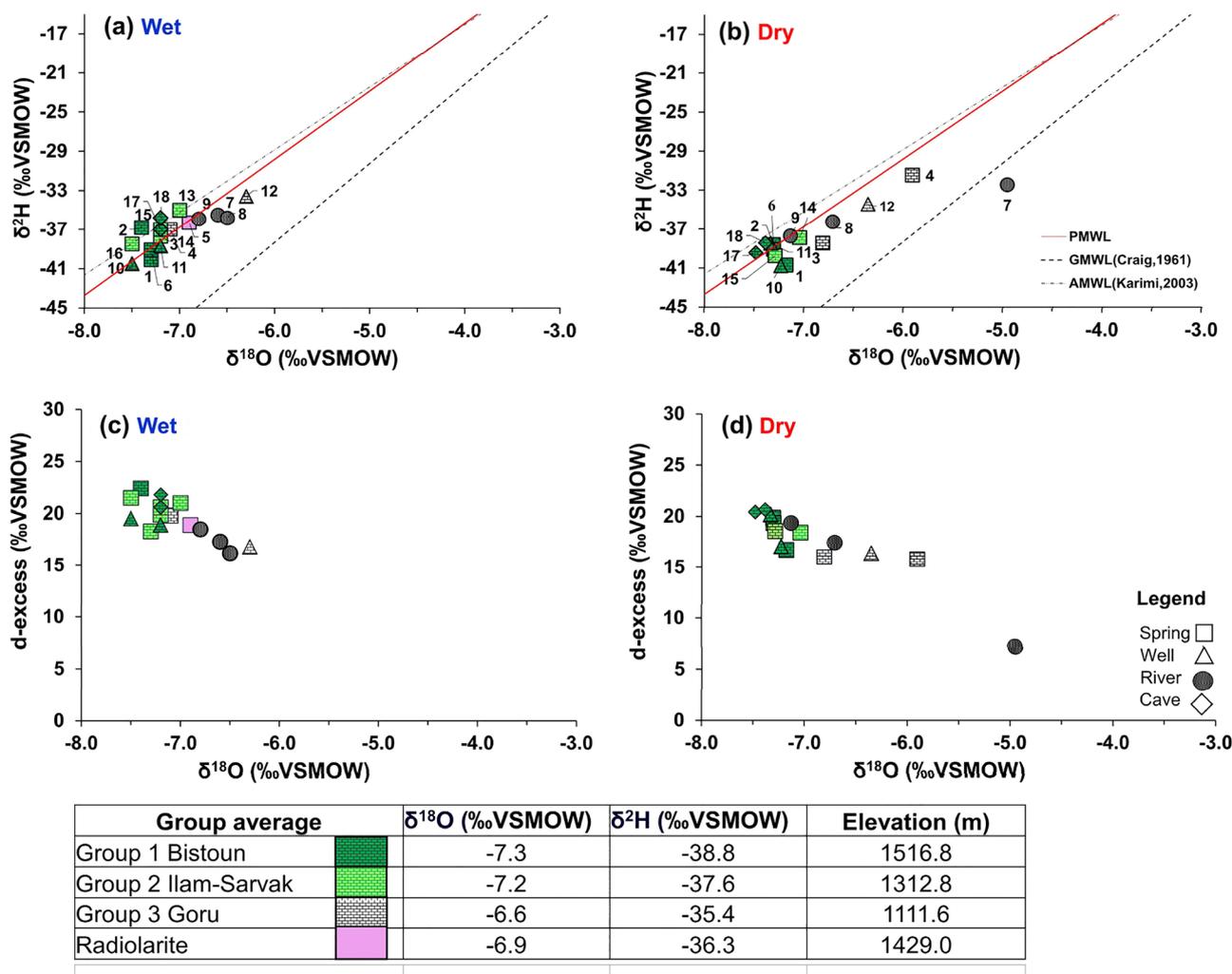


**Fig. 7** a and b The relationship between  $\delta^{18}\text{O}$  and  $\delta^2\text{H}$ , and c and d *d-excess* vs.  $\delta^{18}\text{O}$  in water resources  $\delta$  during the wet and dry seasons (Note: The numbers used in graphs are the locations of sampling sites which are listed in Table S1)

may pass through well-developed karstic formations, which leads to a short residence time of water (Mustafa et al. 2015). It is believed that these samples were recharged at high altitudes during cold seasons, and that is why, they caused such depleted isotopic composition (Fig. 7 c, d). Samples taken from locations 1, 2, 6, and 10 have less isotopic fluctuation during wet and dry seasons, which could refer to the huge amount of base flow in the Bistoun karstic aquifer. Most of the samples in this group are located in the eastern part of the PV–JR area (Fig. 7 a, b).

The second group of water resources with the average isotopic values of  $-7.2$  and  $-37.6$  ‰ for  $\delta^{18}\text{O}$  and  $\delta^2\text{H}$ , correspondingly, is located in Ilam–Sarvak formation (KII-KSv). The average elevation of Ilam–Sarvak water resources is lower than that of Bistoun formation (JKb), which results in low isotopic depletion compared to Bistoun resources. According to Fig. 7a, the precipitations of

the Alvand region in the southern part of the study area are affected by the water resources of the Ilam–Sarvak group and result in placing near and on the AMWL. However, it also seems that these samples were affected by minor evaporation during the dry season (Fig. 7b).

The third group of water resources is categorized under Goru formation (Gr), with the isotopic content of  $-6.6$  and  $-35.4$  ‰ for  $\delta^{18}\text{O}$  and  $\delta^2\text{H}$ , respectively, and is plotted below PMWL. The average elevation of Goru water resources (about 1112 m.a.s.l.) is lower than that of the other groups, and thus, samples have enriched isotopic values, due to more evaporation, which is intensified during the dry season. The low and variable permeability of the aquifer materials in this group could result in longer and different residence times and affect secondary processes such as mixing (Clark and Fritz 1997).

Khaneqah spring (5), with low discharge and placed in radiolarite debris, shows more enriched isotopic values than other springs due to recharging from adjacent enriched surface waters (Fig. S2). The increase in temperature and lack of precipitation in the dry season caused noticeable enrichment by evaporation in rivers' isotope values, especially for the Sirvan River (Fig. 7 a, b). In most of the samples, the *d-excess* values vary between 16.0 to 22.4 ‰, as Mediterranean air masses dominate the region (Fig. 7 c, d).

**$\delta^{13}\text{C}$ -DIC and DIC concentrations of water resources**

The results of DIC concentration and  $\delta^{13}\text{C}$ -DIC isotope compositions are tabulated in Table S5. The average of  $\delta^{13}\text{C}$ -DIC compositions found to be 54.3 mg L<sup>-1</sup> and - 11.07 ‰ VPDB for groundwater, and 54.1 mg L<sup>-1</sup> and - 10.12 ‰ VPDB for surface water samples (Fig. 8a). The slight difference between these values suggests that rivers had been recharged by the groundwater. The  $\delta^{13}\text{C}$ -DIC values generally originate from the organic material decomposition and carbonate mineral dissolution (Kanduč et al. 2012). Based on DIC concentrations and  $\delta^{13}\text{C}$ -DIC values of water samples, three groups of karstifications (well-, moderate-, and less-developed) can be identified in the study area. First group, with low DIC concentration and enriched  $\delta^{13}\text{C}$ -DIC values indicate low water–rock interaction, short residence time, and well-developed karstic aquifer (such as Hooli and Bil springs). The main source of carbon is mainly originated from carbonate dissolution. A little higher enrichment in

Bil spring (Fig. 8 b, c) suggests that carbonate dissolution is the only source of carbon. In the second group of water samples, the DIC concentration is partially higher,; however, the  $\delta^{13}\text{C}$ -DIC values are more depleted, which indicate that C4 plants affected on aquifer and carbon has been originated from both carbonate dissolution and plant decaying (i.e., Bid Miri, Sarkaran, Khaneqah wells in wet season) (Fig. 8 b, c). Third group of samples represent high DIC concentrations and depleted  $\delta^{13}\text{C}$ -DIC values due to C4 plants effect (i.e., Khaneqah, Shamshir, and Oliya springs). The flowing of water from fractured with longer residence time of water and in turn more carbonate dissolution increases the DIC concentration.

Some springs are located in the lands with vegetation coverage, especially prairies (Bas, Bard Zanjir, Shamshir, and Oliya springs—Fig. 8b, c), which proves the C4 plant's effect with more depleted  $\delta^{13}\text{C}$ -DIC values.

The low concentration of DIC in Hanne Quan waterfall in the wet season proves that the wastewater affected this sample which results in a different trend in comparison to other karstic resources. Different plotting position of the rivers could refer to their origination source. Sirvan and Do-Ab Nowsud rivers recharged by well-developed karst resources, while Pavveh River originated from less-developed one or from a far recharging source.

Due to the difference in residence time of water, as well as different temperatures in the wet and dry seasons, samples represent a sort of fluctuation in  $\delta^{13}\text{C}$ -DIC values during the wet and dry season (Fig. 8 b, c).

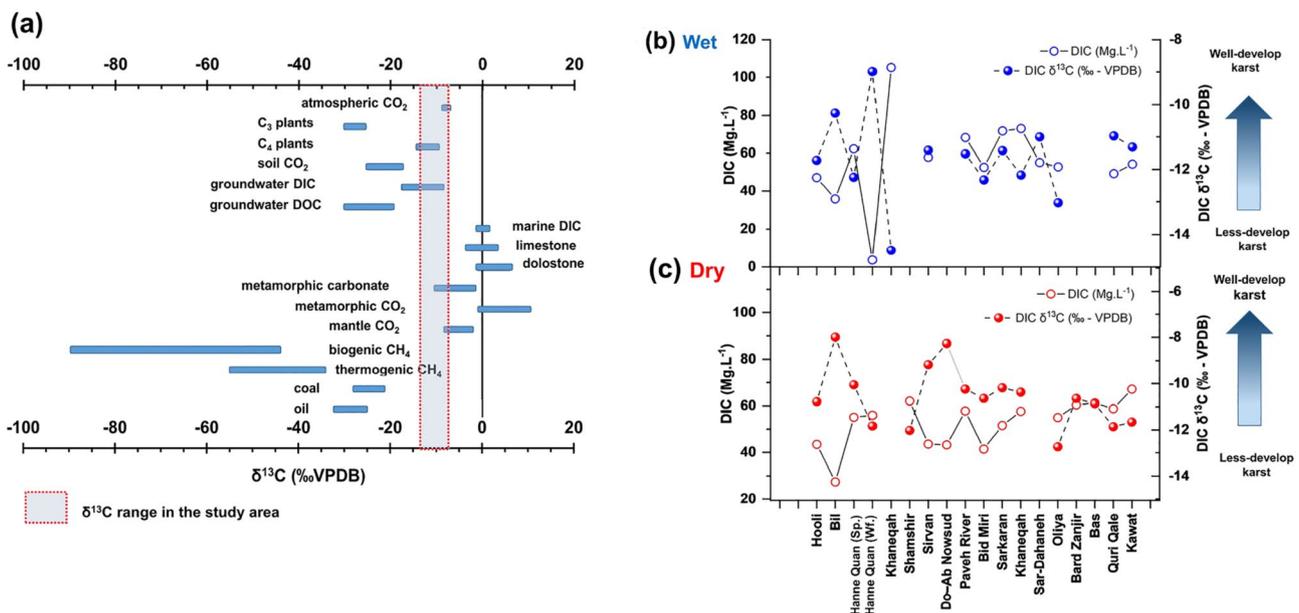


**Fig. 8** a The  $\delta^{13}\text{C}$  ranges for main terrestrial resources, reproduced from (Clark 2015). The connection between DIC concentrations vs.  $\delta^{13}\text{C}$ -DIC (‰ VPDB) in (b) wet and c dry seasons. Note: The num-

bers used in graphs are the locations of sampling sites which are listed in Fig. 1b and S1

## Conclusion

In this study, a combination of multiple environmental tracers such as stable isotopes (including  $\delta^{18}\text{O}$ ,  $\delta^2\text{H}$ , and  $\delta^{13}\text{C}$ ) and hydrochemical techniques were used to study the characteristics of the karstic complex region of the PV–JR area located in northwest (NW) of Iran. Based on the acquired isotopic data of precipitation ( $\delta^{18}\text{O}$  and  $\delta^2\text{H}$ ), hydrochemical investigations, and stable isotopes of water resources, the findings can be briefed as follows: (i) the calculated PV meteoric line (PMWL) equation and water *d-excess* values illustrate that dominant air masses originated from the Mediterranean Sea. Due to the rapid infiltration of meteoric water through the karst aquifer, most water resources are plotted near and on the PMWL, and groundwater recharge happened in cold climatic conditions. (ii) The Piper diagram, correlation matrix, saturation indices (SI), and Gibbs model all indicated that water resources had interactions with pure limestone (Bistoun formation—JKb, as the most well-developed karst system in the PV–JR area) and limestone with some sort of impurity as shale and dolomite (Ilam–Sarvak—KII-KSv) and Goru formation with (gray limes to black shales—Gr) as the less-developed karst systems in the PV–JR area. Bistoun formation (JKb) samples represent lowest TDS (average of  $297 \text{ mg L}^{-1}$ ) and  $\text{SI}_{\text{calcite}}$  (2.5), due to high karst development. Ilam–Sarvak formation (KII-KSv) water samples have moderate TDS (average of  $353 \text{ mg L}^{-1}$ ) and  $\text{SI}_{\text{calcite}}$  (2.6) and Goru formation (Gr) water resources represent the highest TDS ( $368 \text{ mg L}^{-1}$ ) and  $\text{SI}_{\text{calcite}}$  (3.1), due to longer residence time of water. (iii) Regarding  $\delta^{18}\text{O}$  and  $\delta^2\text{H}$  isotopic results, samples are categorized into three groups. First, Bistoun (JKb) water samples with isotopic values of  $-7.3 \text{ ‰}$  and  $-38.8 \text{ ‰}$  for  $\delta^{18}\text{O}$  and  $\delta^2\text{H}$ , respectively, are located in the east part of the region and represent high deplete isotopic values, due to water movement through the well-developed aquifer with short residence time. The second group of water samples are located in Ilam–Sarvak (KII-KSv) formation in the south part of the region and have a bit depleted isotope values ( $-7.2 \text{ ‰}$  and  $-37.6 \text{ ‰}$  for  $\delta^{18}\text{O}$  and  $\delta^2\text{H}$ ) compared to Bistoun water samples. Third, water resources of Goru formation (Gr) ( $-6.6 \text{ ‰}$  and  $-35.4 \text{ ‰}$  for  $\delta^{18}\text{O}$  and  $\delta^2\text{H}$ ) represent enriched isotopic values which are due to high residence time of water in low-permeability aquifer materials. (iv) DIC concentrations and carbon isotope results indicate dissolution of carbonate formations, C4 plants decaying and some sort of (well-, moderate-, and less-developed) karstification in the study area. Some water samples (such as Hooli and Bil springs) with low DIC concentration and enriched  $\delta^{13}\text{C}$ -DIC values show carbonate dissolution and short residence time and well-developed

karstification (i.e.,  $27.4 \text{ mg L}^{-1}$  and  $-7.99 \text{ ‰}$  VPDB in Bil spring). Some other samples have low DIC concentration and, however, more depleted  $\delta^{13}\text{C}$ -DIC values, which carbon has been originated from both carbonate dissolution and C4 plant source (i.e.,  $41.4.8 \text{ mg L}^{-1}$  and  $-10.64 \text{ ‰}$  VPDB in Bid Miri well). A few samples show high DIC concentration and depleted  $\delta^{13}\text{C}$ -DIC values (i.e.,  $52.8 \text{ mg L}^{-1}$  and  $-13.03 \text{ ‰}$  VPDB in Oliya spring), resulted due to the longer residence time of water flowing in fractured carbonate water. Generally, water chemistry (TDS and SI) and isotopic investigations ( $\delta^{18}\text{O}$ ,  $\delta^2\text{H}$ , DIC concentration, and  $\delta^{13}\text{C}$ -DIC isotopic value) all prove that Bistoun formation (JKb) has the most developed karst system and the mean residence time of water is short. The karstic development of Ilam–Sarvak (KII-KSv) formation is less than Bistoun (JKb) and water has a longer residence time. Goru (Gr) water resource characteristics indicate that the karst system is less-developed and water has a longer residence time. The findings of the current study would be beneficial for unraveling the effective management ways of water resources supplied from karstic aquifers in arid and semi-arid areas, which is an undeniable factor for sustainable development.

**Supplementary Information** The online version contains supplementary material available at <https://doi.org/10.1007/s12665-021-09925-8>.

**Acknowledgements** We gratefully thank the Kermanshah's Meteorological Organization, Regional Water Company, Science & Technology Park, and the Ferdowsi University of Mashhad for providing meteorological data and field support. We also acknowledge Dr. Ramon Aravena for his partially financial support, Mr. R. Elgood and Mr. J. Harbin for their technical help in the geochemical and isotopic analyses at the University of Waterloo-Environmental Isotope Laboratory (UW-EIL), Canada, and Dr. Majid Altafi and Mr. Javad Eskandari Mivan for their helps on fieldworks. Finally, the authors appreciate Mr. Mohammadreza Kosari for his grammatical editing.

**Author contributions** EE helped on sampling and field works and drafted the manuscript. HM performed the field works, laboratory analysis, supervised the project, contributed to data-curation, reviewing, and revised the manuscript.

## Declarations

**Conflict of interest** The authors declare no competing financial interest.

## References

- Adeli A, Baghaei F (2013) Production and supply of rainbow trout in Iran and the world. *World J Fish Mar Sci* 5:335–341
- Appelo CAJ, Postma D (2004) *Geochemistry, groundwater and pollution*. CRC Press
- Ayadi Y et al (2018) Hydrochemistry and stable isotopes ( $\delta^{18}\text{O}$  and  $\delta^2\text{H}$ ) tools applied to the study of karst aquifers in Southern

- Mediterranean basin (Teboursouk area, NW Tunisia). *J Afr Earth Sci* 137:208–217
- Barati G, Heydari I (2003). Classification of Iran western precipitation. In: The first Iran National Climate Change Conference; Iran Meteorological Organization: Tehran, Iran, pp 16–23
- Barešić J, Horvatinčić N, Roller-lutz Z, (2011) Spatial and seasonal variations in the stable C isotope composition of dissolved inorganic carbon and in physico-chemical water parameters in the Plitvice Lakes system. *Isotopes Environ Health Stud* 47:316–329
- Barnes RT, Raymond PACG (2009) The Contribution of Agricultural and Urban Activities to Inorganic Carbon Fluxes within Temperate Watersheds. *Chem Geol* 266:318–327
- Barth J, Cronin A, Dunlop J, Kalin R (2003) Influence of carbonates on the riverine carbon cycle in an anthropogenically dominated catchment basin: evidence from major elements and stable carbon isotopes in the Lagan River (N. Ireland). *Chem Geol* 200:203–216
- Belkhir L, Boudoukha A, Mouni L, Baouz T (2011) Statistical categorization geochemical modeling of groundwater in Ain Azel plain (Algeria). *J Afr Earth Sci* 59:140–148
- Bershaw JG (2018) Controls on deuterium excess across Asia. *Geosciences*. <https://doi.org/10.3390/geosciences8070257>
- Cane G, Clark ID (1999) Tracing ground water recharge in an agricultural watershed with isotopes. *Groundwater* 37:133–139
- Clark I (2015) *Groundwater geochemistry and isotopes*. CRC Press
- Craig H (1961) Isotopic variations in meteoric waters. *Science* 133:1702–1703
- Djabri L, Rouabhi A, Hani A, Lamouroux C, Pulido-Bosch A (2008) Origin of water salinity in a lake and coastal aquifer system. *Environ Geol* 54:565–573
- Döll P et al (2012) Impact of water withdrawals from groundwater and surface water on continental water storage variations. *J Geodyn* 59:143–156
- Farid S, Baloch MK, Ahmad SA (2012) Water pollution: major issue in urban areas. *Int J Water Resour Environ Eng* 4:55–65
- Fisher RS, Mullican WF III (1997) Hydrochemical evolution of sodium-sulfate and sodium-chloride groundwater beneath the northern Chihuahuan Desert, Trans-Pecos, Texas, USA. *Hydrogeol J* 5:4–16
- Florea LJ (2010) Isotopes of carbon in a karst aquifer of the Cumberland plateau of Kentucky, USA. *Acta Carsologica*. <https://doi.org/10.3986/ac.v42i2-3.668>
- Florea LJ, McGee DK (2010) Stable isotopic and geochemical variability within shallow groundwater beneath a hardwood hammock and surface water in an adjoining slough (Everglades National Park, Florida, USA). *Isotopes Environ Health Stud* 46:190–209
- Freeze RA, Cherry JA (1979) *Ground water contamination*. Groundwater, Ontario, Canada, pp. 383–456
- Gat JR, Carmi I (1987) Effect of climate changes on the precipitation patterns and isotopic composition of water in a climate transition zone: case of the Eastern Mediterranean Sea area. The influence of climate change and climatic variability on the hydrologic regime and water resources, vol 168. International Association Hydrological Sciences Publication Vancouver, pp 513–523
- Gibbs RJ (1970) Mechanisms controlling world water chemistry. *Science* 170:1088–1090
- Gleick P, Schneider S (1996) *Encyclopedia of climate and weather*. Water Resour 2:817–823
- Goldscheider N, Drew D (2014) *Methods in karst hydrogeology: IAH: international contributions to hydrogeology*, 26. CRC Press, Boca Raton
- Gonfiantini R, Sauzay G, Payne B, Conrad G, Fontes JC (1974) Isotopic study of the continental intercalaire aquifer and its relationship with other aquifers of the northern Sahara. In: *Isotope techniques in groundwater hydrology 1974, Vol I. Proceedings of a symposium*
- Grossman EL (1997) Stable carbon isotopes as indicators of microbial activity in aquifers. In: Hurst CJ, Knudsen GR, McInerney MJ, Stetzenbach LD, Walter MV (eds) *Manual of Environmental Microbiology*. ASM Press, Washington, DC, pp 565–576
- Hamamin DF, Ali SS (2013) Hydrodynamic study of karstic and intergranular aquifers using isotope geochemistry in Basara basin Sulaimani, North-Eastern Iraq. *Arab J Geosci* 6:2933–2940
- Han D, Liang X, Jin M, Currell M, Song X, Liu C (2010a) Evaluation of groundwater hydrochemical characteristics and mixing behavior in the Daying and Qicun geothermal systems, Xinzhou Basin. *J Volcanol Geotherm Res* 189:92–104
- Han G, Tang Y, Wu Q (2010b) Hydrogeochemistry and dissolved inorganic carbon isotopic composition on karst groundwater in Maolan, southwest China. *Environ Earth Sci* 60:893–899
- Han Z, Tang C, Wu P, Zhang R, Zhang C (2014) Using stable isotopes and major ions to identify hydrological processes and geochemical characteristics in a typical karstic basin, Guizhou, southwest China. *Isotopes Environ Health Stud* 50:62–73
- Heald D, Looij E, Bunting T, Patten J (2007) *Surface water sampling methods and analysis. Technical appendices: standard operating procedures for water sampling methods and analysis*. Government of western Australia, department of water
- Hounslow A (2018) *Water quality data: analysis and interpretation*. CRC Press
- Jiang Y, Cao M, Yuan D, Zhang Y, He QJHJ (2018) Hydrogeological characterization and environmental effects of the deteriorating urban karst groundwater in a karst trough valley: Nanshan, SW China. *Hydrogeol J* 26:1487–1497
- Jin J, Zimmerman AR, Moore PJ, Martin JB (2014) Organic and inorganic carbon dynamics in a karst aquifer: Santa Fe River Sink-Rise system, north Florida, USA. *J Geophys Res Biogeosci* 119:340–357
- Kanduč T, Mori N, Kocman D, Stibilj V, Grassa F (2012) Hydrogeochemistry of alpine springs from north Slovenia: insights from stable isotopes. *Chem Geol* 300:40–54
- Karimi H, Raeisi E, Bakalowicz M (2005) Characterising the main karst aquifers of the Alvand basin, northwest of Zagros Iran, by a hydrogeochemical approach. *Hydrogeol J* 13:787–799
- Khazaei M, Byzedi M (2016) Climate change impact on annual meteorological and hydrological variables of the Sirvan Basin. *Iran Water Resour Res* 12(2):38–48
- Knierim KJ, Pollock E, Hays PD (2013) Using isotopes of dissolved inorganic carbon species and water to separate sources of recharge in a cave spring, northwestern Arkansas, USA Blowing Spring Cave. *Acta Carsologica*. <https://doi.org/10.3986/ac.v42i2-3.667>
- Kumar PS, Elango L, James E (2014) Assessment of hydrochemistry and groundwater quality in the coastal area of South Chennai, India. *Arab J Geosci* 7:2641–2653
- Langmuir D (1997) *Aqueous environmental geochemistry*, No. 551.48 L3. Prentice Hall, Upper Saddle River, New Jersey
- Liu F, Wang S, Wang L, Shi L, Song X, Yeh TCJ, Zhen P (2019) Coupling hydrochemistry and stable isotopes to identify the major factors affecting groundwater geochemical evolution in the Heilongdong Spring Basin, North China. *J Geochem Explor* 205:106352
- Marques JM, Eggenkamp HG, Graça H, Carreira PM, José Matias M, Mayer B, Nunes D (2010) Assessment of recharge and flowpaths in a limestone thermomineral aquifer system using environmental isotope tracers (Central Portugal). *Isotopes Environ Health Stud* 46:156–165
- Mohajjel M, Fergusson CIGR (2014) Jurassic to Cenozoic tectonics of the Zagros Orogen in northwestern Iran. *Int Geol Rev* 56:263–287
- Mohammadzadeh H, Aravena RPEPS (2015) Investigating the origin and interaction between Karstic and Alluvial Aquifers in NW of Zagros Mountain range, Iran, using isotopic and geochemical tools. *Procedia Environ Sci* 13:256–260

- Mohammadzadeh H, Ebrahimpour S (2012) Application of stable isotope and hydrogeochemistry to investigate the origin and water resources' quality variations in Zarivar lake Cathment area. *Water Soil* 26(4):1018–1031
- Mohammadzadeh H, Eskandari E (2018) Application of hydrogeochemical and isotopic techniques for better understanding of water resources characteristics in Paveh and Javanrud study areas, Kermanshah. *Hydrogeology* 3:80–98
- Mohammadzadeh H, Heydarizad M (2020) A conceptual model for water resources circulation patterns in Andarokh-Kardeh region (NE, Iran). *Geochemistry*. <https://doi.org/10.1016/j.chemer.2019.125593>
- Mohammadzadeh H, Eskandari Mayvan J, Heydarizad M, Meteorology P (2020) The effects of moisture sources and local parameters on the  $^{18}\text{O}$  and  $^2\text{H}$  contents of precipitation in the west of Iran and the east of Iraq. *Tellus B Chem Phys Meteorol*. <https://doi.org/10.1080/16000889.2020.1721224>
- Morsali M, Rezaei M (2017) Assessment of  $\text{H}_2\text{S}$  emission hazards into tunnels: the Nosoud tunnel case study from Iran. *Environ Earth Sci*. <https://doi.org/10.1007/s12665-017-6493-0>
- Mustafa O, Merkel B, Weise S (2015) Assessment of hydro geochemistry and environmental isotopes in karst springs of Makook anticline, Kurdistan region, Iraq. *Hydrology* 2:48–68
- Odriscoll M, DeWalle D, McGuire K, Gburek W (2005) Seasonal  $^{18}\text{O}$  variations and groundwater recharge for three landscape types in central Pennsylvania, USA. *J Hydrol* 303:108–124
- Osati K, Koeniger P, Salajegheh A, Mahdavi M, Chapi K, Malekian A (2014) Spatiotemporal patterns of stable isotopes and hydrochemistry in springs and river flow of the upper Karkheh River Basin, Iran. *Isotopes Environ Health Stud* 50:169–183
- Ozdemir A, Nalbantcilar TM (2002) The investigation of mass transfer in the Karasu karstic aquifer, Konya, Turkey. *Hydrogeol J* 10:656–661
- Parisi S et al (2011) Groundwater recharge areas of a volcanic aquifer system inferred from hydraulic, hydrogeochemical and stable isotope data: mount vulturne, southern Italy. *Hydrogeol J* 19:133–153
- Parkhurst DL (1995) User's guide to PHREEQC: A computer program for speciation, reaction-path, advective-transport, and inverse geochemical calculations. vol 95, No. 4227. US Department of the Interior, US Geological Survey
- Pavlovskiy I, Selle B (2015) Integrating hydrogeochemical, hydrogeological, and environmental tracer data to understand groundwater flow for a karstified aquifer system. *Groundwater* 53:156–165
- Qin D et al (2017) Using hydrochemical, stable isotope, and river water recharge data to identify groundwater flow paths in a deeply buried karst system. *Hydrol Process* 31:4297–4314
- Raziei T, Bordi I, Pereira LJH, Sciences ES (2008) A precipitation-based regionalization for western Iran and regional drought variability. *Hydrol Earth Syst Sci Discuss* 12:1309–1321
- Sadeghi S, Yassaghi ASE (2016) Spatial evolution of Zagros collision zone in Kurdistan NW Iran: constraints on Arabia-Eurasia oblique convergence. *Solid Earth* 7:659–659
- Sánchez D, Andreo B, López M, González M, Mudarra M (2015) Characterization of carbonate aquifers (Sierra de Grazalema, S Spain) by means of hydrodynamic and hydrochemical tools. *Hydrogeological and environmental investigations in karst systems*. Springer, Berlin, pp 171–180
- Sappa G, Vitale S, Ferranti F (2018) Identifying karst aquifer recharge areas using environmental isotopes: a case study in central Italy. *Geosciences* 8:351
- Stumm W, Morgan JJ, Morgan JJ (1981) *Aquatic Chemistry*. A Wiley-Interscience-Publication, New York
- Toft P, Malaiyandi M, Hickman J (1987) *Guidelines for Canadian drinking water quality*. American Chemical Society, Washington
- World Health Organization (1993) *Guidelines for drinking-water quality*. World Health Organization
- Xuan Y, Cao Y, Tang C, Li M (2020) Changes in dissolved inorganic carbon in river water due to urbanization revealed by hydrochemistry and carbon isotope in the Pearl River Delta, China. *Environ Sci Pollut Res*. <https://doi.org/10.1007/s11356-020-08454-4>
- Zarei P, Talebi A, Alaie Taleghani MJE (2018) Sensitivity analysis of effective factors in hillslopes instability; a case study of Javanrud region, Kermanshah province. *Ecopersia* 6:259–268

**Publisher's Note** Springer Nature remains neutral with regard to jurisdictional claims in published maps and institutional affiliations.